ORIGINAL RESEARCH

Local delivery of controlled-release simvastatin to improve the biocompatibility of polyethylene terephthalate artificial ligaments for reconstruction of the anterior cruciate ligament

Peng Zhang[1,*]
Fei Han[2,*]
Yunxia Li[1]
Jiwu Chen[1]
Tianwu Chen[1]
Yunlong Zhi[1]
Jia Jiang[1]
Chao Lin[2]
Shiyi Chen[1]
Peng Zhao[2]

[1]Department of Sports Medicine, Huashan Hospital, Fudan University; [2]Shanghai East Hospital, The Institute for Biomedical Engineering and Nanoscience, School of Medicine, Tongji University, Shanghai, People's Republic of China

*These authors contributed equally to this work

Correspondence: Shiyi Chen; Peng Zhao
Department of Sports Medicine, Huashan Hospital, Fudan University, 12 Middle Wulumuqi Road, Shanghai 200040, People's Republic of China
Tel +86 21 5288 8255
Fax +86 21 6249 6020
Email chenshiyifudan@sina.com; zp@tongji.edu.cn

Abstract: The Ligament Advanced Reinforcement System has recently been widely used as the primary graft of choice in anterior cruciate ligament (ACL) reconstruction. But the biological graft–bone healing still remains a problem. Previous studies have shown that simvastatin (SIM) stimulates bone formation. The objective of this study was to investigate whether surface coating with collagen containing low-dose SIM microsphere could enhance the surface biocompatibility of polyethylene terephthalate (PET) artificial ligaments to accelerate graft-to-bone healing. The in vitro studies demonstrated that bone marrow stromal cells on the collagen-coated PET scaffolds (COL/PET) and simvastatin/collagen-coated PET scaffolds (SIM/COL/PET) proliferated vigorously. Compared with the PET group and the COL/PET group, SIM could induce bone marrow stromal cells' osteoblastic differentiation, high alkaline phosphatase activity, more mineralization deposition, and more expression of osteoblast-related genes, such as osteocalcin, runt-related transcription factor 2, bone morphogenetic protein-2, and vascular endothelial growth factor, in the SIM/COL/PET group. In vivo, rabbits received ACL reconstruction with different scaffolds. Histological analysis demonstrated that graft–bone healing was significantly greater with angiogenesis and osteogenesis in the SIM/COL/PET group than the other groups. In addition, biomechanical testing at the eighth week demonstrated a significant increase in the ultimate failure load and stiffness in the SIM/COL/PET group. The low dose of SIM-sustained release from SIM/COL/PET promoted the graft–bone healing via its effect on both angiogenesis and osteogenesis. This study suggested that collagen containing low-dose SIM microsphere coating on the surface of PET artificial ligaments could be potentially applied for ACL reconstruction.

Keywords: simvastatin, controlled release, graft–bone healing, biocompatibility, ligament reconstruction

Introduction

Anterior cruciate ligament (ACL) rupture is a common and devastating sports-related knee injury. The annual incidence of the ACL injury is 35 of 100,000 people of all ages, and >120,000 ACL reconstructions are performed annually in the United States.[1–4] The ACL provides an essential mechanism for ensuring knee stability and normal knee kinematics.[5] Surgical reconstruction of the ACL is often recommended, particularly in young and active patients. Presently, the three categories of commonly used grafts in ACL reconstruction are autograft, allograft, and synthetic graft (such as artificial or xenograft). Graft choice for ACL reconstruction is influenced by the patient's age, activity level, sex, associated injuries, degree of laxity, and planned concomitant

operations.[6] Autografts usually consist of either four-strand hamstring grafts (double semitendinosus and gracilis tendon grafts), bone–patella tendon–bone, or the quadriceps tendons. However, the autograft also has drawbacks, such as donor site morbidity, unlimited availability, and longer recovery times, while the allografts carry the possibility of disease transmission and infection. Processed xenografts can be considered as another option. But their effectiveness is still under debate.[7] Currently, the most widely accepted synthetic graft is the Ligament Augmentation Reconstruction System (LARS; Surgical Implants and Devices, Arc-sur-Tille, France), which comprises fibers made of polyethylene terephthalate (PET).[8,9] LARS artificial ligament introduced the "soft tissue fixation" concept; short-term and medium-term follow-up showed satisfactory clinical effect. However, similar to many polymeric or metallic implants, LARS ligaments can cause serious side-effects such as poor tendon–bone healing, bolt loose, and synovitis.[10,11] The LARS artificial ligament graft has not yet reached the real "ligamentization" after ACL reconstruction surgery. The PET ligament material is hydrophobic and chemically inert and has poor biological properties. Therefore, the improvement of the biocompatibility and postoperative "ligamentization" of PET ligament are still under study.

Simvastatin (SIM), which was developed as a 3-hydroxy-3-methylglutaryl-CoA reductase inhibitor, has been widely used for the treatment of dyslipidemia and the prevention of cardiovascular diseases.[12–14] Mundy et al[15] reported that SIM and lovastatin have strong bone anabolic effects that were attributed to the induction of the bone inducing factor bone morphogenic protein-2 (BMP-2).[16] Previous studies found that the SIM can also elicit some pleiotropic effects, such as endothelial effect, anti-inflammatory effect, and stimulation of angiogenesis.[17–19] The effects of SIM may be influenced by a range of factors, including the administration method, exposure duration, animal model, and bioavailability. High systemic (oral) administration of SIM presents a limited positive effect on bone healing due to the associated systemic toxicities.[20] In contrast, local delivery of SIM has been reported to have a positive effect on bone formation.[21–24] Furthermore, Cui et al reported that SIM can mobilize mesenchymal stem cells migrating to bone defects. Because of these properties, SIM can be used as an osteogenic growth factor.[25]

Bioactive coatings are frequently used to improve the biocompatibility of materials. Previous studies showed that we can modify the graft surface property by coating with biocompatible, cytophilic, osteoinductive molecules or hydrophilic natural polymers.[26,27] Therefore, we hypothesized that if we combined a biocompatible collagen coating with low-dose SIM microsphere, this coating might enhance the biocompatibility of PET artificial ligament graft, and the SIM microsphere can release low-dose SIM in a sustainable manner to promote bone regeneration (Figure 1). The purpose
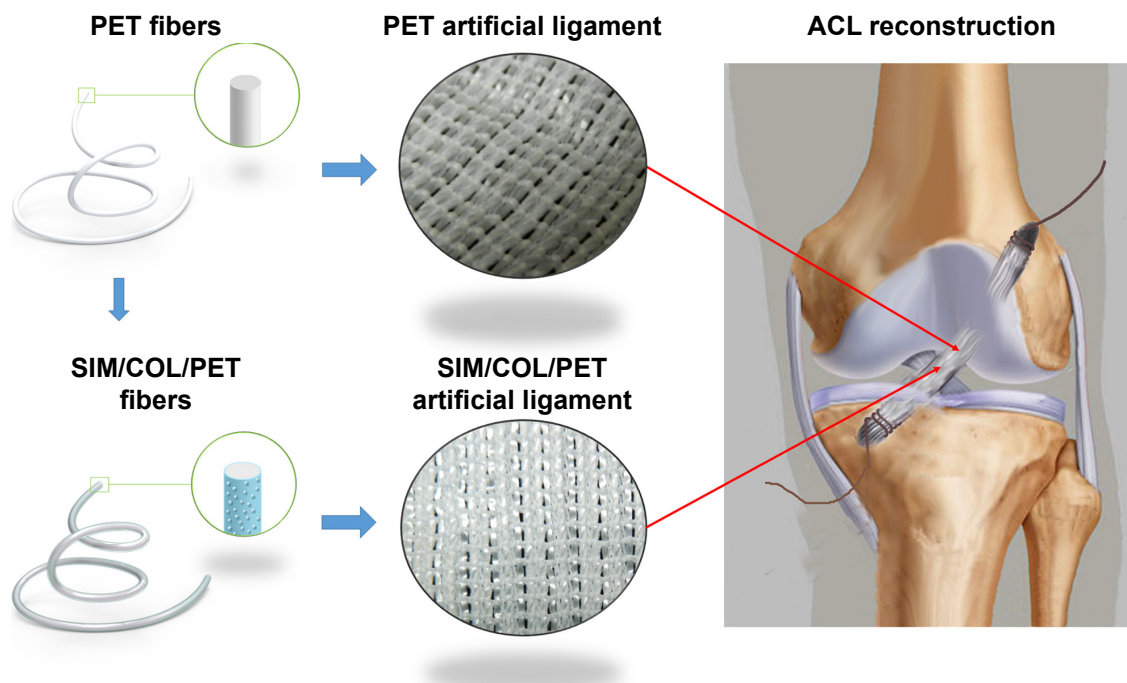
Figure 1 Schematic illustration of PET artificial ligament and collagen/simvastatin microspheres coating on PET in the artificial ligament anterior cruciate ligament (ACL) reconstruction.
Abbreviations: PET, polyethylene terephthalate; SIM/COL/PET, collagen and simvastatin microspheres collagen coating on polyethylene terephthalate fibers.

of this study was to investigate the effects of locally applied SIM/collagen coating on the PET artificial ligament after ACL reconstruction.

Materials and methods
Preparation of SIM/polycaprolactone microspheres

Poly (ε-caprolactone) (PCL, 1 mg/mL) and SIM (10 μg/mL) were dissolved in methylene chloride; the ratio of SIM to PCL was 1:99. The SIM/PCL solution was slowly added dropwise into 8% polyvinyl alcohol solution while high-speed stirring. After high-speed stirring for 30 minutes, low-speed agitation of 100 rpm for 5 hours was performed to volatilize dichloromethane. After 5,000 rpm centrifugation, the polyvinyl alcohol solution was removed. The precipitated solid was washed twice with water, repeated centrifugation and washing, and separated three times, and the sample was frozen, dried, and preserved at 4°C.

Preparation of the PET samples

PET samples were divided into three groups: PET group, COL/PET group, and SIM/COL/PET group. PET sheets and grafts were taken from a LARS ligament (Surgical Implants and Devices). They were prepared and cleaned in the 75% (v/v) alcohol solution to remove contamination and then washed with a large amount of deionized water. The PET samples were modified through plasma surface modification (HPD-100B Plasma Apparatus, Coronalab Co. Ltd, Nanjing, People's Republic of China) at power 80 W and pressure 25 Pa for 15 seconds. SIM/PCL microspheres were dispersed in the 3 mg/mL rat-tail collagen solution, the concentration of the microspheres in the collagen solution was 1 μg/mL, and the pH value was adjusted to 7.5 by NaOH. The plasma-treated PET samples were immersed in the rat-tail collagen/SIM microspheres solution for 20 minutes at low temperatures. Thereafter, the samples were placed in a centrifuge tube and incubated in sterile phosphate-buffered saline (PBS) at 37°C for 30 minutes. The obtained samples were named as SIM/COL/PET group. According to the same method, the plasma-treated PET samples were immersed in the rat-tail collagen solution. The obtained samples were named as COL/PET group.

Structural characterization

The SIM/COL/PET group, COL/PET group, and PET group specimens were observed with a scanning electron microscope (SEM) (Vega3, Tescan Co. Ltd, Brno, Czech Republic). The samples were vacuum coated with gold, placed in the vacuum chamber of the electron microscope, and viewed at 20 keV accelerating voltage. The overall morphology of the SIM/PCL microsphere was also examined using SEM. The particle size and particle size distribution were calculated by particle size analysis (LS-230, Beckman Coulter, Fullerton, CA, USA).

Water contact angle was measured by a Model 200 video-based optical system (Future Scientific Ltd Co., Taiwan, People's Republic of China) to investigate the hydrophilicity of different PET scaffolds. PET sheets were treated according to the earlier method. A water drop of 1 μL in volume was used to wet the PET sample surface, and the water–sample interaction was seen through the video recorder of the instrument. Images of the water–sample interaction were obtained, and the contact angle was computed using the VCA Optima software.

Drug release

The in vitro release profile of SIM was determined by UV spectrophotometry. The 50 mg SIM/polycaprolactone microspheres were dispersed in 50 mL sterile PBS solution and incubated at 37°C. The wavelength of 238 nm solution (1 mL/day) was detected by ultraviolet spectrophotometer. According to the standard curve, the daily amount of sustained release was converted once a day for the next 30 days. The cumulative drug release rate was calculated as being:

$$\text{Cumulative drug release rate} = \frac{\text{Mass of released drug}}{\text{Mass of total drug}}$$

In vitro experiments
Isolation and expansion of bone marrow stromal cells

All animal-handling procedures were performed according to the Guide for the Care and Use of Laboratory Animals of the National Institutes of Health and followed the guidelines of the Animal Welfare Act. All animal experiments were approved by the Institutional Animal Care and Use Committee of Fudan University. Bone marrow stromal cells (BMSCs) were extracted and isolated from tibia and femur bone marrow of Kunming mice (n=3). The cells were cultured in an alpha-modified Eagle's medium (Sigma-Aldrich Co., St Louis, MO, USA) supplemented with 10% fetal bovine serum (HyClone Logan, UT, USA), L-glutamine (580 mg/L), and penicillin–streptomycin (100 U/mL). The cells were cultured at 37°C in an incubator with 5% CO_2 incubator. The medium was changed every other day.

Cell proliferation and adherence

The treated PET films and control group were cut into 1.0 cm diameter wafer and adhered to 24-well plates by rat-tail col-

lagen. Each well was added to 1 mL Dulbecco's Modified Eagle's Medium (DMEM) and 1 mL cell suspension (5,000/mL). After 1 day, 3 days, 5 days, 7 days, and 9 days culturing, the activity of the cells was detected using the cell-counting kit-8 (CCK-8) according to the manufacturer's instructions (Dojindo Laboratories, Kumamoto, Japan). The optical density value was determined at 540 nm by a spectrophotometer (MK3, Thermo Fisher Scientific, Waltham, MA, USA). BMSCs were seeded on the treated and untreated samples in 24-well plates; each well was inoculated with 1 mL cell suspension (100,000/mL). After 8 hours of culture, the samples were removed to a new culture plate and culturing was continued. Residual cells at the bottom of the well were called "lost cells". Twenty-four hours later, the samples were vibrated in an orbital shaker for 10 minutes. Some cells were washed away from the surface of the samples; these cells are called "inadhesive cells". The inadhesive cells were collected, and the residual cells in the original wells were collected by trypsinization. The ratio between the lost/inadhesive cells and the total amount of seeded cells was calculated, respectively. The cell morphology and distribution were visualized under SEM. BMSCs were seeded on the samples and cultivated for 8 hours, 1 day, and 4 days, respectively. Specimens were fixed in 0.25% glutaraldehyde solution for 4 hours, and then rinsed three times in PBS. Subsequently, the specimens were dehydrated in increasing concentrations of acetone (30%–100% v/v). After drying, the specimens were mounted on aluminum stubs and coated with gold and then viewed under a SEM (Vega3).

Alkaline phosphatase activity of SIM-induced BMSCs

The osteogenic effects of PET, COL/PET, and SIM/COL/PET on BMSCs were evaluated using ALP activity assays. The PET, SIM/COL/PET, and COL/PET sheets were pasted at the bottom of 24-well plates by rat-tail collagen, respectively. BMSCs (1×10^5 cells/well) were seeded onto different PET sheets and cultured in osteogenic induction medium (OIM), in the presence of 10 mM β-glycerol phosphate (Sigma-Aldrich), 0.1 mM dexamethasone (Sigma-Aldrich), and 50 mg/mL ascorbic acid (Sigma-Aldrich) supplemented in DMEM–high glucose medium containing 10% (v/v) fetal bovine serum and 1% (v/v) penicillin–streptomycin. In the control groups, BMSCs were seeded in the 24-well plates. The negative control group was cultured with common DMEM. In the positive control group, the cells were first cultured in DMEM for 1 day. The medium was then replaced with OIM. After 3 days and 7 days, the osteogenic differentiation of the cells

was evaluated by alkaline phosphatase (ALP) staining and ALP quantitative analysis using an ALP kit according to the manufacturer's protocol.

Mineralization assays for SIM-induced BMSCs

Alizarin red S staining was used to determine the level of calcification in the extracellular matrix. BMSCs (1×10^5 cells/well) were seeded in 24-well plates and cultured for 24 hours. The PET, SIM/COL/PET, and COL/PET sheets were pasted at the bottom of the 24-well plates by rat-tail collagen, respectively, and then replaced with OIM for another 21 days. The cells were fixed in 10% formalin and PBS for 10 minutes. After washing twice with double-distilled H_2O, the fixed cells were stained with Alizarin red S solution for 5 minutes. After staining, the cells were washed using double-distilled H_2O. The fixed and stained plates were then air-dried at room temperature. The amount of mineralization was determined by dissolving the cell-bound Alizarin red S in 10% acetic acid and measured at 415 nm. The value was normalized to total protein in each well. The total protein in the cells was lysed in PhosphoSafe™ reagent (Novagen, Darmstadt, Germany). Protein concentrations were determined using the Bio-Rad protein assay (Bio-Rad Laboratories Inc., Hercules, CA, USA). The detection wave length was 415 nm. This test was repeated three times.

Real-time polymerase chain reaction analysis

Total RNA was extracted from the cells cultured in the PET specimens by TRIzol (Thermo Fisher Scientific) at the first day and the third day. The extracted RNA was used to generate the complementary DNA using reverse transcriptase Moloney murine leukemia virus (D2640A; Takara, Beijing, People's Republic of China) according to the manufacturer's instructions. Expression of osteogenic genes, BMP-2, osteocalcin (OC), runt-related transcription factor 2 (RUNX-2), vascular endothelial growth factor (VEGF), and β-actin was evaluated. Quantitative polymerase chain reaction (PCR) was performed with SYBR Premix Ex Taq (DRR041A; Takara) and then detected by a real-time (RT) PCR system (TP800; Takara, Kyoto, Japan). Two hundred nanograms of total RNA was reverse transcribed into complementary DNA. The messenger RNA levels of BMP-2, VEGF, RUNX-2, and OC were normalized to the expression of an endogenous housekeeping gene, β-actin, using the delta–delta Ct method. The primers were designed as follows: BMP-2 forward 5′-AGCTGCAAGAGACACCCTTTG-3′ and reverse 5′-AGCATGCCTTAGGGATTTTGGA-3′;

RUNX-2 forward 5′-CCCAGCCACCTTTACCTACA-3′ and reverse 5′-TATGGAGTGCTGCTGGTCTG-3′; OC forward 5′-GAGGGCAATAAGGTAGTGAACA-3′ and reverse 5′-AAGCCATACTGGTCTGATAGCTCG-3′; VEGF forward 5′-CCATGAACTTTCTGCTCTTC-3′ and reverse 5′-GGTGAGAGGTCTAGTTCCCGA-3′; β-actin forward 5′-CCAACCGTGAAAAGATGACC-3′ and reverse 5′-ACCAGAGGCATACAGGGACA-3′.

The PCR condition was as follows: 95°C for 5 minutes, 40 cycles of 30 seconds at 95°C, 30 seconds at 68°C, and 60 seconds at 72°C. Each RT-PCR run was performed with at least three experimental replicates, and the results are presented as target gene expression normalized to β-actin.

In vivo experiments

ACL reconstruction animal model

Institutional Animal Care and Use Committee of Fudan University approved all animal trials. Thirty-six adult New Zealand White rabbits with average weight of 2.5–3.5 kg underwent an operative ACL reconstruction procedure (Figure 2B) on their left limbs. The rabbits were randomly divided into three groups: PET group, COL/PET group, and SIM/COL/PET group. The ACL reconstruction was performed under strictly aseptic conditions. Anesthesia was induced by the intravenous administration of 3% pentobarbital (30 mg/kg body weight). The animal was placed supine on the operating table. The left limb was disinfected before skin incisions were made. The lateral parapatellar arthrotomy was used to expose the left knee joint of the rabbit. The native ACL was exposed and removed from the insertion sites by sharp dissection. The bone tunnels were created with the use of a 2.5 mm diameter drill in the femur and tibia insertion sites of the native ACL. The graft was passed through the bone tunnel and joint cavity. Both ends of the grafts were attached to the adjacent periosteum and soft tissue with two 4-0 Ethibond sutures (Johnson & Johnson, New Brunswick, NJ, USA), and then the wound was closed layer by layer. The rabbits were kept in the cages for their free activities after surgical procedure. The animals were, respectively, sacrificed at the fourth- and eighth-week postsurgery to harvest tissue specimens for histological and biomechanical analyses.
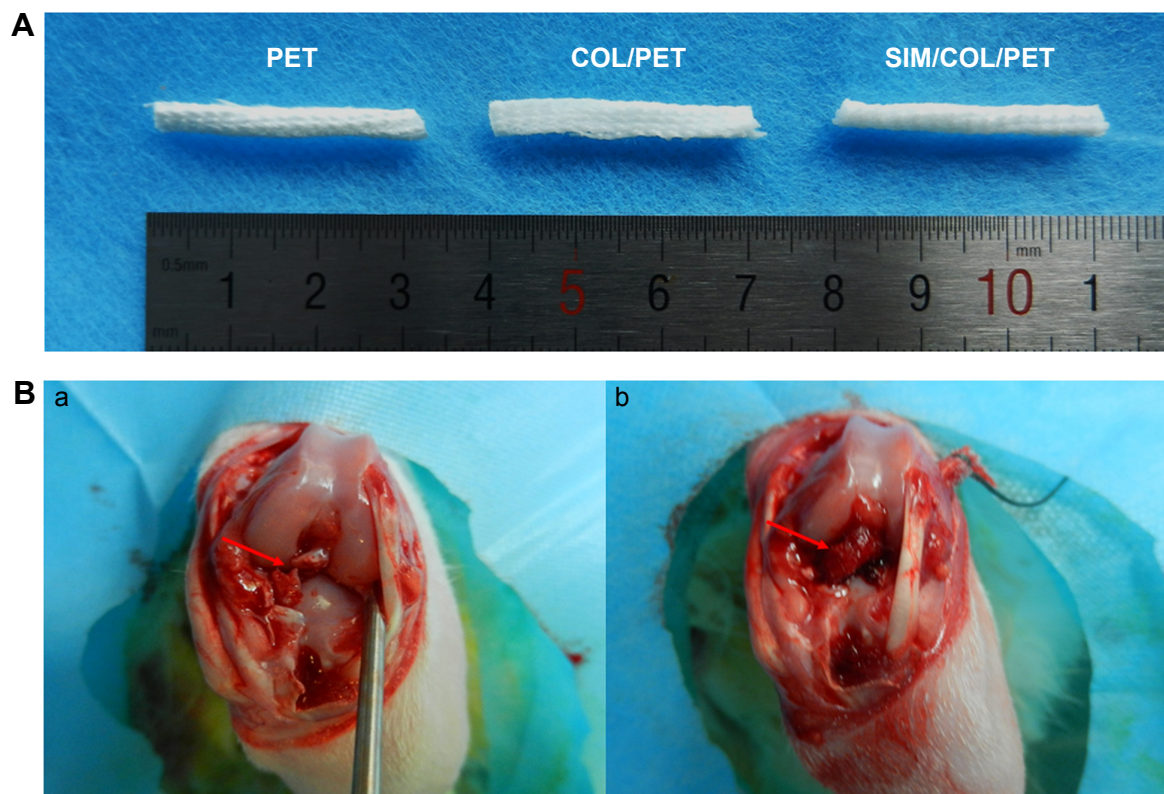
Figure 2 Digital images of the grafts and ACL reconstruction operation.
Notes: (**A**) Gross observation of PET, COL/PET, and SIM/COL/PET scaffolds. (**B**, a) Macroscopic view of rabbit knee joint (the arrow points to ACL rupture). (**B**, b) Macroscopic view of ACL reconstruction (the arrow points to implant).
Abbreviations: PET, polyethylene terephthalate; COL/PET, collagen coating on polyethylene terephthalate scaffolds; SIM/COL/PET, collagen and simvastatin microspheres coating on polyethylene terephthalate scaffolds; ACL, anterior cruciate ligament.

Histological and immunohistological assessments

Immediately after sacrifice, the femur–implant–tibia complexes were fixed in 10% neutral buffered formalin for 48 hours and then embedded undecalcified in a methyl methacrylate compound according to established protocols. The samples were sectioned perpendicularly to the longitudinal axis of the tibial tunnel with a thickness of 5 μm by using a microtome (SM2500; Leica Microsystems, Wetzlar Germany). These sections were stained with hematoxylin and eosin stain for histological evaluation. The graft–bone interface was visualized by inverted light microscopy (IX71SBF2; Olympus Corporation, Tokyo, Japan), and the digital images were taken using a DP72 Manager (Olympus Corporation). For immunohistochemistry staining, endogenous peroxidase was blocked by incubation with 3% (v/v) hydrogen peroxide in methanol for 10 minutes. After washing three times with PBS, the sections were blocked with blocking reagent containing goat serum in PBS for 20 minutes. After overnight incubation at 4°C with primary antibody (rabbit anti-human VEGF, diluted 1:50; Bioworld), the sections were washed and then incubated with a secondary antibody (MaxVision kit; Maixin Biotechnology) for 15 minutes at room temperature. The dimethyl aminoazobenzene (DAB) (Simple Stain DAB Solution, Maixin Biotechnology, Shanghai, People's Republic of China) was used for color development. Hematoxylin staining was used to reveal the nuclei. The results were evaluated by three individuals who were blinded to the treatments.

Mechanical testing

The specimens (n=5 limbs in each group at each time point) were harvested from each knee after sacrifice and prepared for mechanical testing immediately without being frozen. All soft tissues, except for the ACL graft, were carefully removed from the femur–graft–tibia complex. All mechanical testing was conducted using an electronic universal materials testing system machine (AGS-X, Shimadzu, Co., Japan). Before the tensile test, the samples were preloaded with a static preload of 1 N for 5 minutes. After preconditioning, the ultimate failure load was carried out immediately with an elongation rate of 2 mm/min. The load–deformation curve was recorded from which the ultimate failure load (N) was measured. Stiffness (N/mm) was calculated from the slope of the linear region of the load–deformation curve at the maximal load-to-failure point. For each sample, the test was completed when the graft was ruptured or pulled out of the bone tunnel.

Statistical analysis

All data were expressed as mean ± standard deviation. Student's t-test was performed to assess statistically significant differences in the results of different experimental groups. Comparisons of groups at different time points were performed using an independent two-sample Student's t-test. Comparisons of numerical data among multiple groups were performed by one-way analysis of variance (ANOVA), least significant difference (LSD) t-test. Statistical analysis was carried out using SPSS Statistics 18.0 statistical software package, and $P<0.05$ was considered statistically significant.

Results
Structural characterization

Significant differences cannot be found between the PET, COL/PET, and SIM/COL/PET grafts (Figure 2A), but the SEM analysis revealed their different microstructures. SEM imaging of the PET grafts showed a smooth surface before plasma pretreatment (Figure 3A). After surface coating with SIM/collagen, the PET ligament surfaces appeared to be rougher in comparison to PET without coating, and hydrogel-like materials were seen on the fiber surface (Figure 3D). It meant that the coating of SIM/collagen significantly changed the external morphology of the ligaments by refining the roughness of the surface. In the SIM/COL/PET group, a large number of microspheres were effectively adhered to the surface of the PET samples (Figure 3G), and the SEM imaging of the microspheres is shown in Figure 4A. In addition, ~85% of the SIM/polycaprolactone microspheres were within the size range of 0.7–1.5 μm, and the average particle diameter was 1.1±0.15 μm. The collagen coating will promote cell adherence, while the SIM microsphere coating will promote migration and differentiation in the bone tunnels by releasing SIM slowly. To investigate the change in wettability of the PET samples, the water contact angle was measured before and after the application of the collagen and SIM coating (Figure 4C). There was a statistical significant difference in the water contact angle among the PET group (85.25±5.19), COL/PET group (33.68±1.94), and SIM/COL/PET group (34.11±2.12) ($P<0.05$). Obviously, the collagen coating played a very important role in improving the hydrophilicity of PET. We reasoned that collagen/SIM coating should effectively modify the wettability of the PET scaffold.

SIM release kinetics in vitro

The in vitro release profile of SIM from SIM microspheres graft in PBS was analyzed by UV spectrophotometry. The data, which appear in Figure 4B, showed initial burst release (0%–21.5%) over the first 3 days. The encapsulation efficiency of SIM in SIM/polycaprolactone microspheres was
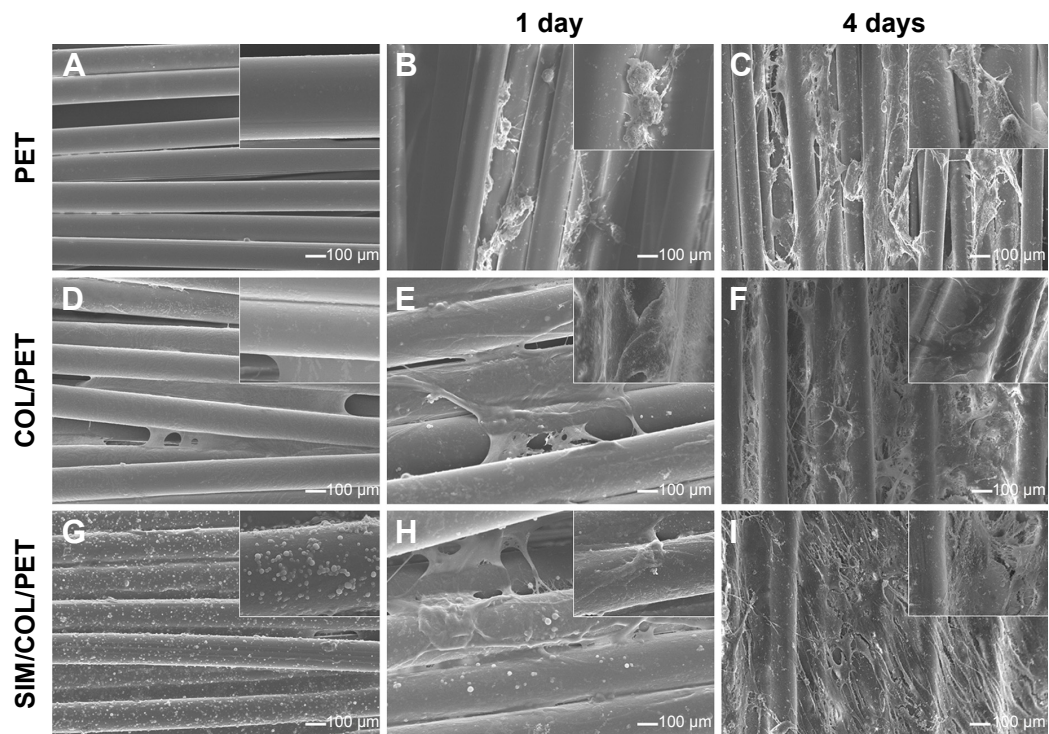
Figure 3 Scanning electron microscopic images of morphologic changes and cell adhesion in different fibers at 1 day and 4 days (100× magnification).
Notes: Micromorphology: original PET fibers (**A**), COL/PET (**D**), SIM/COL/PET (**G**); BMSCs adhesion: PET (**B**, **C**), COL/PET (**E**, **F**), and SIM/COL/PET (**H**, **I**). Insets show magnified sections of **A-I** (10× magnification).
Abbreviations: PET, polyethylene terephthalate; COL/PET, collagen coating on polyethylene terephthalate scaffolds; SIM/COL/PET, collagen and simvastatin microspheres coating on polyethylene terephthalate scaffolds; BMSCs, bone marrow stromal cells.
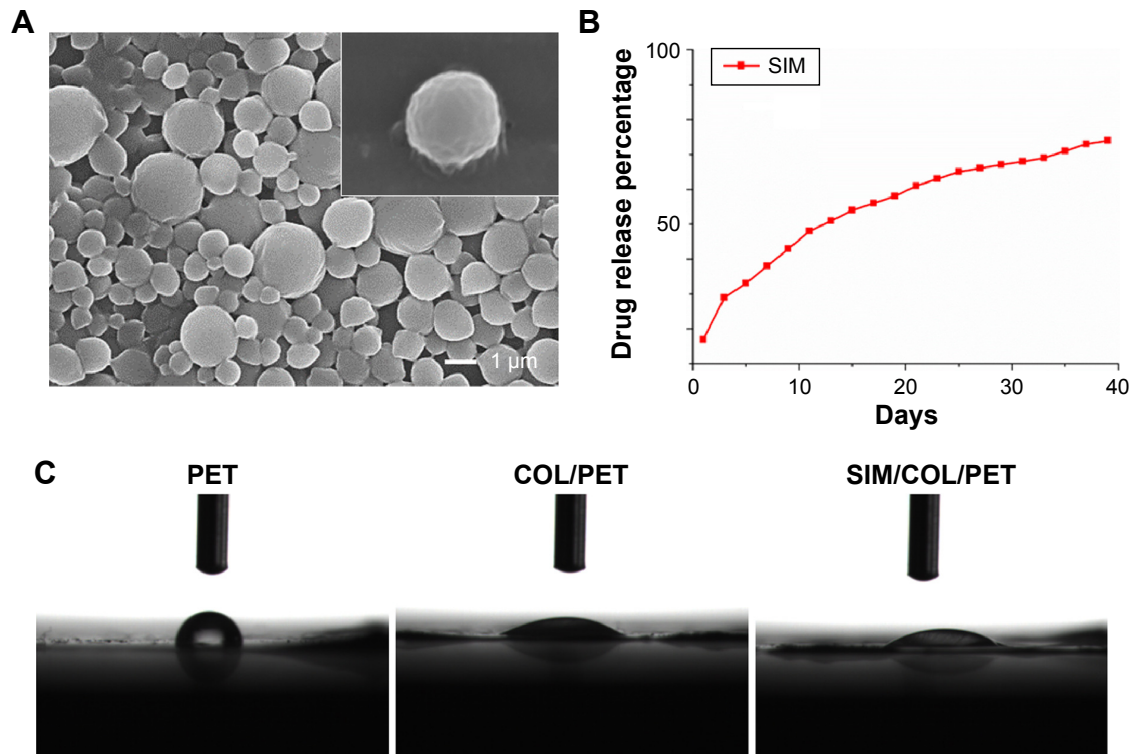
Figure 4 Characterization of the PET coating.
Notes: (**A**) Morphology characterization of simvastatin/polycaprolactone (SIM/PCL) microspheres. Inset shows the morphology of a single microsphere. (**B**) Simvastatin release profiles for SIM/PCL microspheres. (**C**) Water contact angle images of PET (85.25°±8.19°), COL/PET (33.68°±4.94°), and SIM/COL/PET (34.11°±6.12°).
Abbreviations: PET, polyethylene terephthalate; COL/PET, collagen coating on polyethylene terephthalate scaffolds; SIM/COL/PET, collagen and simvastatin microspheres coating on polyethylene terephthalate scaffolds; SIM, simvastatin.

73.1%±11.9%. The cumulative amount of SIM released was >50% of the total concentration after 14 days of release (Figure 4B).

Cell viability and adhesion

Proliferation and viability of the BMSCs were estimated using the CCK-8 kits. As shown in Figure 5B, BMSC proliferation in the SIM/COL/PET group was found to be better than the PET group in CCK-8 assay from 24 hours to 120 hours. The cell morphology on the graft was observed by SEM. The BMSCs grew along the pore walls or fibers and exhibited semi-ovoid or spindle-shaped morphology after seeding on the COL/PET graft and SIM/COL/PET graft (Figure 3E, F, H, I). Although dead cells were not observed, the cells were difficult to grow on and adhere to the PET graft (Figure 5A). BMSCs were seeded on the PET samples for 8 hours. The number of the "lost cells" and "inadhesive cells" on PET samples was the most in the three groups. Adhesion and viability of the cell were better in the COL/PET group and SIM/COL/PET group compared with the PET group. The results suggested that the SIM/collagen coating was biocompatible and provided more space for the cells to grow, thereby promoting cell proliferation and migration.

Osteogenic effect of SIM

The content of ALP may directly reflect the activity or function of osteoblasts. The higher content of ALP suggests that the mineralization capacity of cells is stronger. Specific ALP expression of all groups varied with culturing duration (Figure 6A). As shown in the figure, the higher the content of ALP, the deeper the blue. After staining and quantitative analysis, the content of ALP in the PET group was rare and

the content of ALP in the COL/PET group was higher. In the SIM/COL/PET group, the content of ALP was significantly increased higher compared with the other two groups. The ALP quantitative results showed that the SIM/COL/PET group showed significantly higher degrees of BMSC mineralization compared with the PET group (Figure 6C; $P<0.05$). Osteogenic differentiation assay confirmed that most of the cells had mineralized calcium deposits after 21 days of induction as shown by Alizarin red staining (Figure 6B). According to the results of Alizarin red staining, the COL/PET group and SIM/COL/PET group had more mineralization deposition compared to the PET group. Moreover, the mineralized deposition of the SIM/COL/PET group is significantly more than the other two groups. Although the collagen coating can promote cell mineralization, the significant effect was observed after adding SIM microsphere. This was also showed in the Alizarin red staining quantitative analysis (Figure 6D). Additionally, the gene expression of ligament repair markers, including OC and RUNX-2, was higher than the PET group (Figure 6E and F). In addition, the slow release of SIM increased the expression of the growth factors VEGF and BMP-2 in BMSCs, which were the major regulators of angiogenesis and osteogenesis (Figure 6E and F).

Histological analysis

As shown in Figure 7A, inflammatory cells infiltrated the graft–bone interface in the PET, COL/PET, and SIM/COL/PET groups at 4 weeks after surgery. Thick fibrous scar tissue had formed at the graft-to-bone interface in the PET group and COL/PET group. In the SIM/COL/PET group, there was aligned connective tissue, newly formed
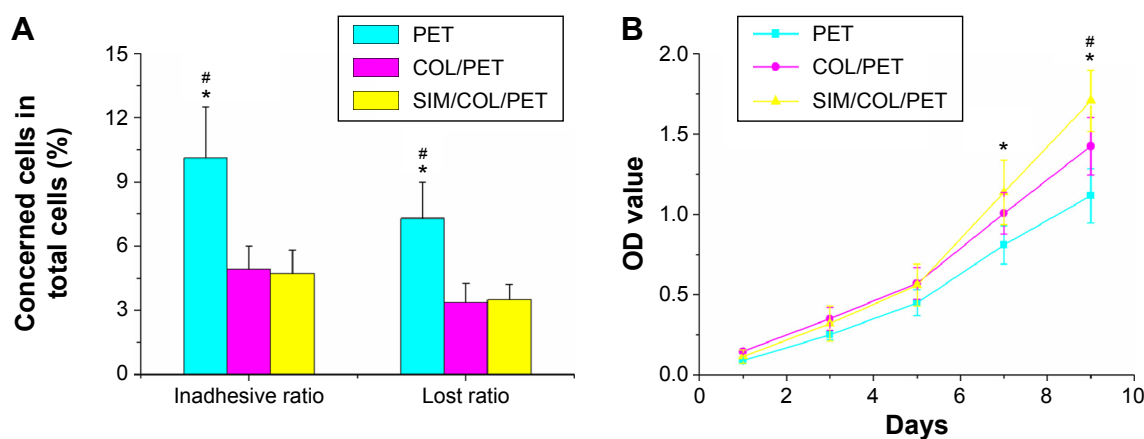

Figure 5 Measurement of BMSC proliferation and adhesion among the PET group, COL/PET group, and SIM/COL/PET group.
Notes: (**A**) Cell adhesion ability on different samples and (**B**) BMSC viability in the scaffolds was detected with cell counting kit-8 (CCK-8). *$P<0.05$ compared with control; #$P<0.05$ between treatment groups.
Abbreviations: PET, polyethylene terephthalate; COL/PET, collagen coating on polyethylene terephthalate scaffolds; SIM/COL/PET, collagen and simvastatin microspheres coating on polyethylene terephthalate scaffolds; BMSC, bone marrow stromal cell; OD, optical density.
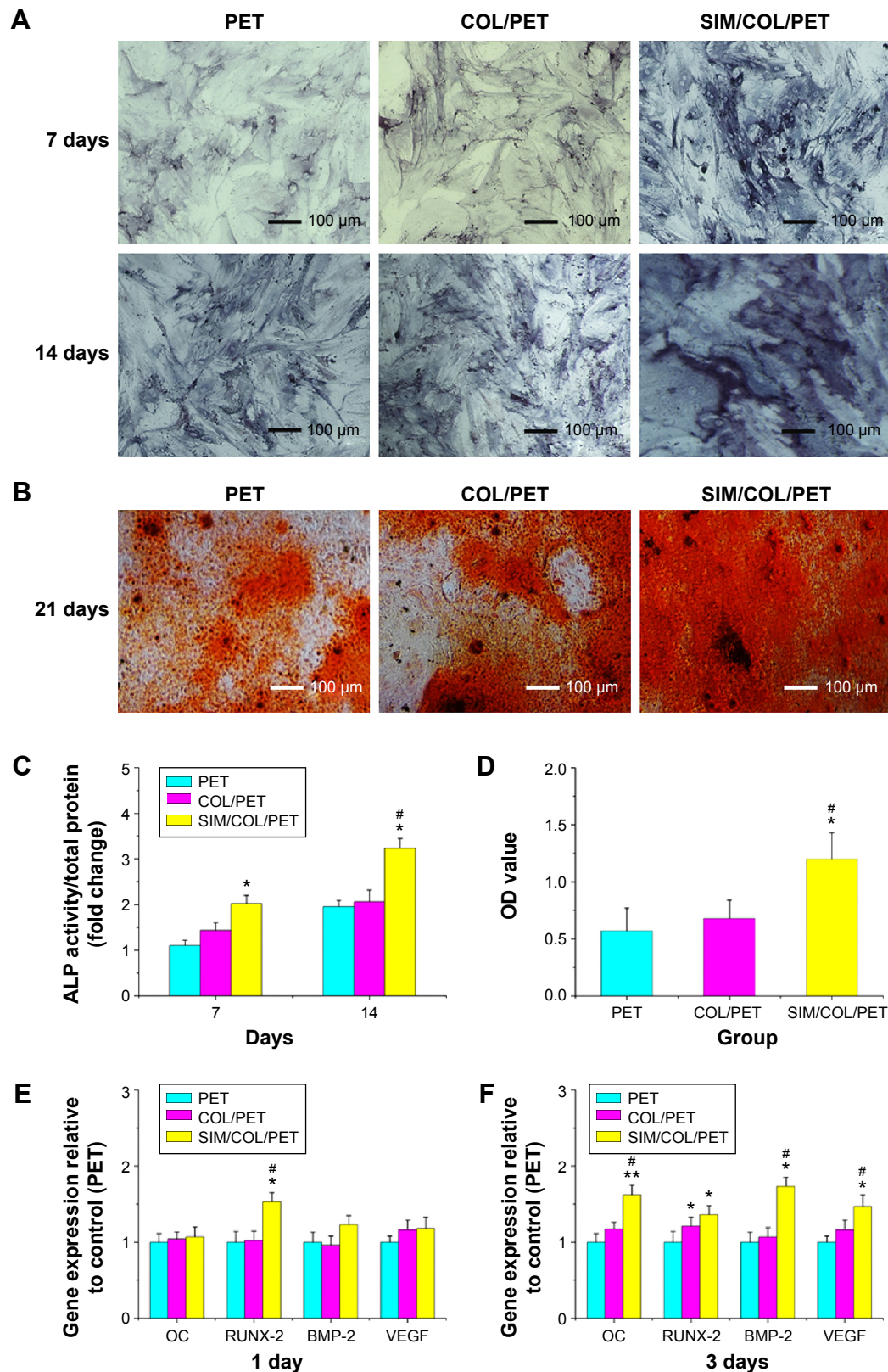
Figure 6 The results of the mineralization of BMSCs seeding on PET samples.
Notes: (**A**) The ALP activity of BMSCs seeded on PET, COL/PET, and SIM/COL/PET scaffolds for 7 days and 14 days. (**B**) Alizarin red staining after BMSCs seeded on these scaffolds for 21 days. (**C**) The ALP quantitative analysis for 7 days and 14 days. (**D**) Alizarin red staining quantitative analysis (415 nm) for 21 days. The osteogenic-related gene expressions (OC, RUNX-2, BMP-2, VEGF) in different groups at days 1 (**E**) and 3 (**F**). *$P<0.05$; **$P<0.01$ compared with control; #$P<0.05$ between treatment groups.
Abbreviations: PET, polyethylene terephthalate; COL/PET, collagen coating on polyethylene terephthalate scaffolds; SIM/COL/PET, collagen and simvastatin microspheres coating on polyethylene terephthalate scaffolds; BMSCs, bone marrow stromal cells; ALP, alkaline phosphatase; BMP-2, bone morphogenetic protein-2; RUNX-2, runt-related transcription factor 2; OC, osteocalcin; VEGF, vascular endothelial growth factor; OD, optical density.
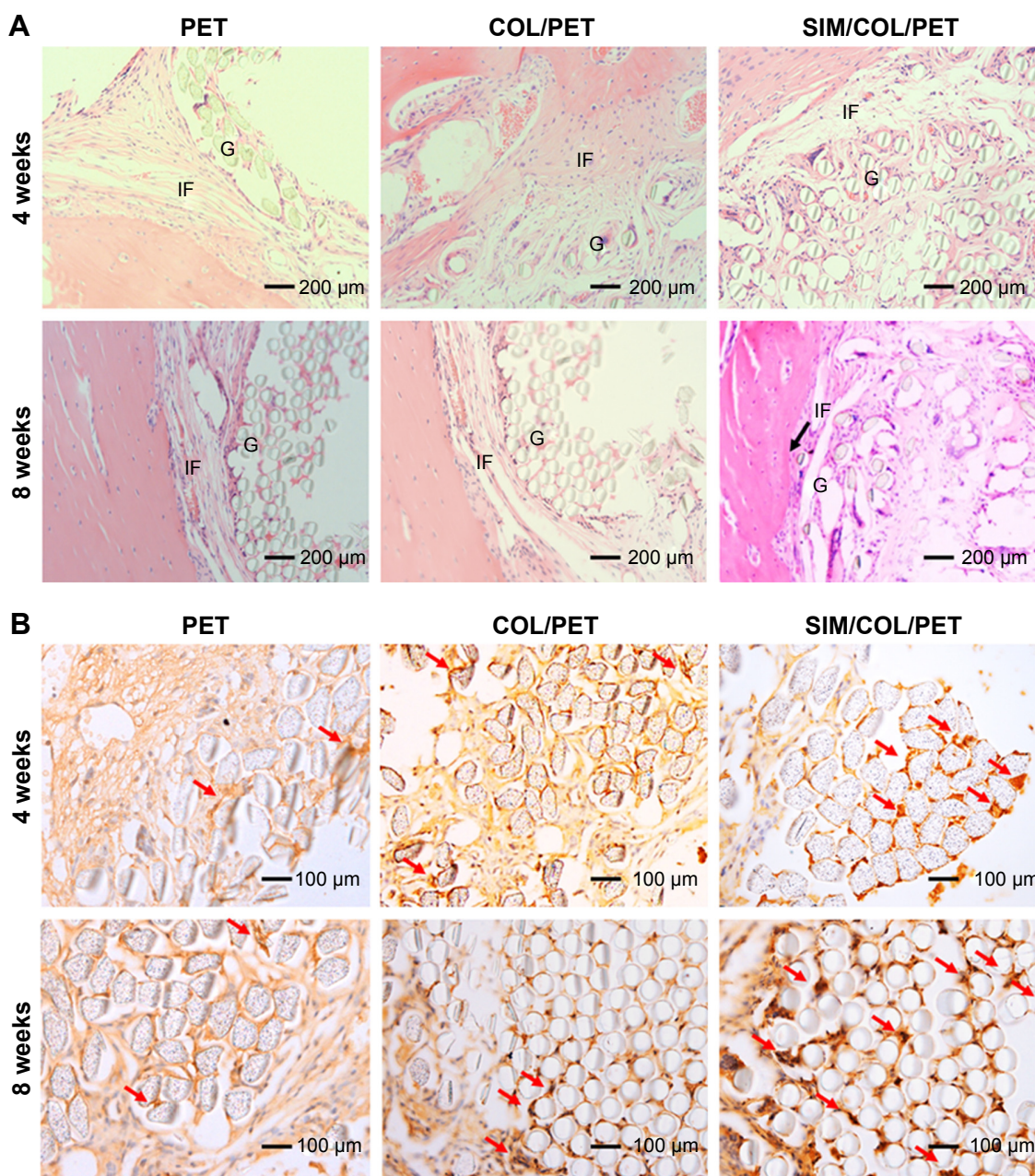
**Figure 7** Histological and immunohistological assessments.
Notes: (**A**) Hematoxylin and eosin staining evaluation of the graft–bone interface at 4 weeks and 8 weeks after surgery (magnification, ×200). The black arrow shows the tendon–bone interface. (**B**) Immunohistochemical staining of the osteogenic and angiogenesis marker, VEGF, at 4 weeks and 8 weeks after surgery (magnification, ×100). The brown precipitate represented stained VEGF (red arrows).
Abbreviations: G, artificial ligament graft; IF, interface; VEGF, vascular endothelial growth factor; PET, polyethylene terephthalate; COL/PET, collagen coating on polyethylene terephthalate scaffolds; SIM/COL/PET, collagen and simvastatin microspheres coating on polyethylene terephthalate scaffolds.

woven bone, and cartilage in the tendon–bone interface. At 8 weeks after surgery, some protruding new bone tissue formation was found at the interface between host bone and graft in the SIM/COL/PET group, while a thick fibrous tissue band was observed in the PET group and COL/PET group. Furthermore, compared with the other two groups, the results of hematoxylin and eosin staining showed that the width of graft–bone interface became much narrower than the other two groups in the SIM/COL/PET group,

and no significant difference was found between the COL/PET group and PET group (Figure 7A). It meant that the biocompatibility of the SIM/COL/PET group was better. The immunohistochemical staining of the osteogenic and angiogenesis marker, VEGF, is shown in Figure 7B. The brown precipitate represented stained VEGF, and the content of VEGF in the SIM/COL/PET group was higher. This meant that the SIM/COL/PET group had a higher level of vascularization.
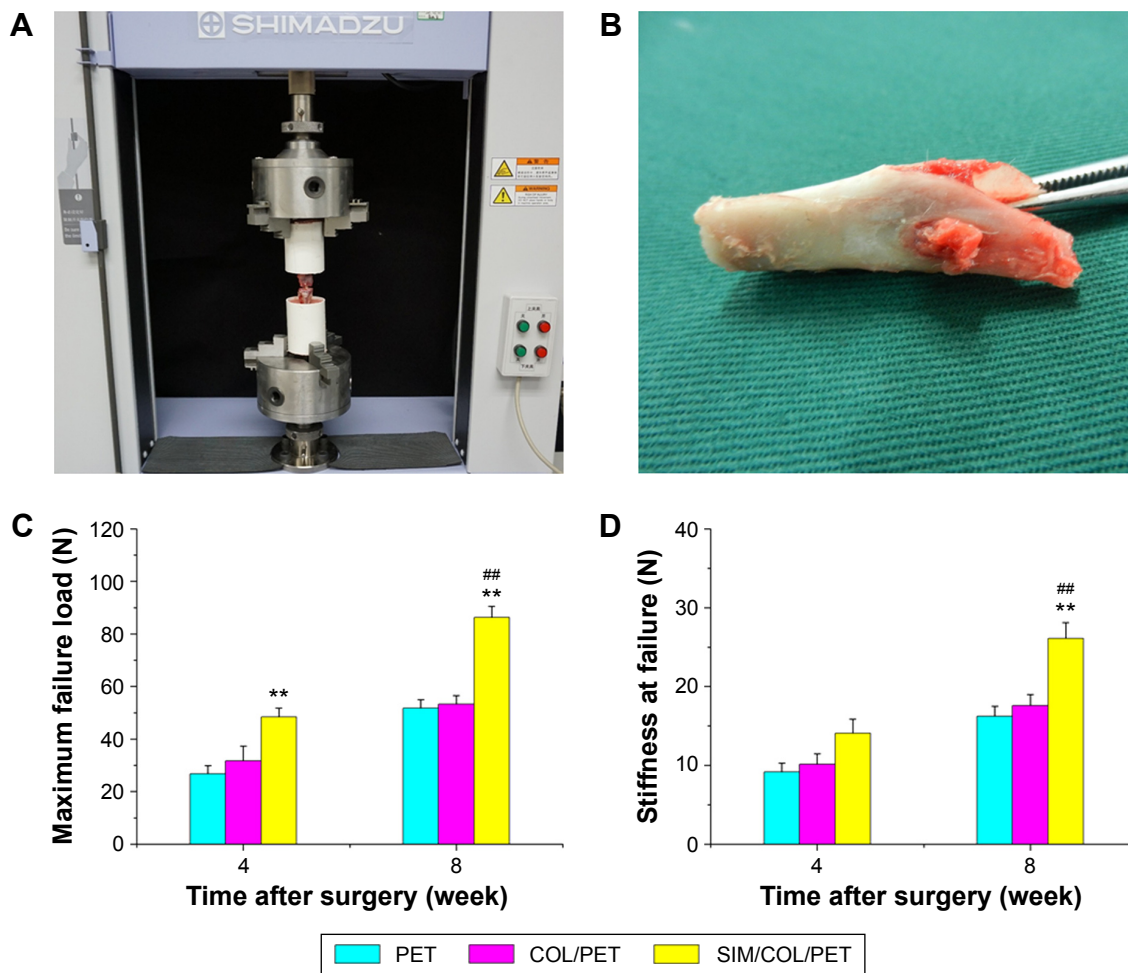
Figure 8 Mechanical examinations for graft–bone healing in a rabbit model at each time point after surgery.
Notes: (**A**) Digital camera image of biomechanical test experiment of implanted graft. (**B**) PET graft was in the tibial bone tunnel. (**C**) Comparison of maximal failure load among the PET group, COL/PET group, and SIM/COL/PET group. (**D**) Comparison of stiffness at failure among the PET group, COL/PET group, and SIM/COL/PET group. **P<0.01 compared with control; ##P<0.01 between treatment groups.
Abbreviations: PET, polyethylene terephthalate; COL/PET, collagen coating on polyethylene terephthalate scaffolds; SIM/COL/PET, collagen and simvastatin microspheres coating on polyethylene terephthalate scaffolds.

Biomechanical testing

All specimens failed by pullout from the tunnel at 4 weeks and 8 weeks. No graft rupture occurred. After 4 weeks, although the load to failure in the SIM/COL/PET group was significant higher than that in the PET group, there was no statistically significant difference in the load to failure between the COL/PET and SIM/COL/PET groups (P=0.2031). After 8 weeks, the mean load to failure of the SIM/COL/PET group was higher than that of the COL/PET group (86.4±4.1 N vs 53.4±3.1 N, respectively; P<0.01) (Figure 8C). There were no significant differences in stiffness between the COL/PET group and SIM/COL/PET group at 4 weeks (14.0±2.0 N/mm vs 10.0±1.7 N/mm; P=0.0181). After 8 weeks, the average stiffness in the SIM/COL/PET group was significantly greater than that in the PET group (26.1±2.0 N/mm vs 16.2±1.3 N/mm; P<0.01) and COL/PET group (26.1±2.0 N/mm vs 17.5±1.4 N/mm; P<0.01) (Figure 8D).

Discussion

The successful reconstruction of ACL relies on adequate healing of the graft/bone tunnel interface and reconstructed tissues to withstand the forces transmitted to the native ACL during the knee joint activity. The ACL graft tendon–bone healing and the intra-articular ligamentization process are influenced by many factors, including surgical technical variables such as graft placement, graft length within the bone tunnel, graft fixation, graft tensioning, graft–tunnel micromotion, and the tunnel biologic environment. However, the principal form of healing that occurs in the bone tunnels is primarily dependent on the graft used. The LARS artificial ligament, made of PET material, was deemed the best choice of artificial ligament graft. However, the disadvantage of the PET ligament is hydrophobic, chemical inertness, and poor biocompatibility. Moreover, the surface morphology of a graft plays an important role in cellular attachment,

proliferation, and differentiation. To overcome this disadvantage of the PET ligament, researchers attempted to use the bioactive coatings and surface modification methods for improving graft biocompatibility. Several techniques have been used to modify the surface of synthetic biomaterial scaffolds such as plasma treatment, chemical methods, UV irradiation, and co-electrospinning of active agents and polymers.[28] Nanoparticle-based coating is also an effective strategy that can increase wettability, roughness, and the effective surface area of materials. Nano-microspheres are probably the largest category of nanosized particles used in the drug delivery field. Even more, PCL have been widely used for the preparation of microspheres.[29] Because the surface functionalization (surface chemistry and energy) of biomaterial scaffolds can influence the cells in vitro behavior, the combination of surface coating and drug-loaded nanoparticle technology is a strategy to improve the interaction between the scaffolds' surface and the culturing cells. The drug-loaded nanoparticle coating will consistently enhance functional bonding between the graft and host bone tissue and also promote biomaterial-driven bone regeneration through increased protein adsorption and nutrient exchange.

Based on the earlier facts, in this study, we fabricated a low-dose SIM/collagen coating to modify the surface of PET artificial ligament grafts. Collagen has been widely used as a material for protein and drug delivery or as a scaffold since it is particularly biocompatible, well established, safe, and biodegradable and it enhances cellular penetration in the extracellular matrix formation.[30] The SIM/COL/PET scaffold can release SIM in a sustainable manner and significantly enhance osteogenesis in BMSC cultures. This is the first reported study demonstrating that a coating can release SIM in a sustainable manner to improve bioactivity of the graft for ACL reconstruction surgery.

In an in vitro study, the PET graft surface was modified by the low-temperature plasma. After the material surface modification, we observed (by SEM) that many BMSCs adhered to the SIM/collagen-modified films, while few cells adhered to the pure PET films. In our study, CCK-8, ALP activity, matrix mineralization, and RT-PCR analyses all showed that the proliferation and osteogenic differentiation of BMSCs in the SIM/COL/PET group significantly improved compared to the PET group. SIM/collagen coating could enhance the graft biocompatibility and thereby facilitate BMSCs proliferation and increase osteogenic protein adsorption on the graft surface.

Grafted tendon-to-bone tunnel healing is largely dependent on the new bone formation around tendon grafts.

Therefore, researchers attempted to augment biological healing of tendon-to-bone interface using growth factors, cell-based therapies, and various other delivery and inducement methods. According to various animal model studies, the osteoinductive growth factors, including BMP, transforming growth factor, and fibroblast growth factor, have positive effects on the repair and healing of tendon and bone tissues.[31–36] BMP-2 plays an important role in bone regeneration procedures. However, there are some disadvantages such as their short life, storage and handling difficulties, complicated synthesis, inefficiency in the recognition of target cells, and expensiveness in its application.[37,38] SIM is considered a statin suitable for bone growth activation. Previous studies have shown that SIM reduces osteoclast and increases osteoblast activity and accelerates bone formation locally.[39,40] Zhou et al[41] reported that SIM significantly increased BMP-2, Cbfa1, VEGF, and fibroblast growth factor-2 mRNA expression. Furthermore, SIM can enhance the expression of BMP-2. This unique characteristic was found in other statin-induced cells such as BMSCs or MC3T3-E1.[15,41–44] In our study, SIM significantly stimulated osteogenic gene expression of RUNX-2, BMP-2, ALP, and OC (Figure 6) and final mineralization (Figures 6 and 7) in the SIM/COL/PET groups. This result indicates that the SIM/collagen coating can modify the surface of the PET artificial ligament grafts. Moreover, the release of SIM by the coating may be advantageous for providing an initial stimulation of the local cells to express BMP-2, which can directly induce osteoblastic differentiation by driving the expression of Cbfa1.[41]

The delivery system for SIM is very important because the effectiveness of SIM depends on the rhythm in which the carrier releases the drug, as well as on its local concentration. High systemic (oral) administration of SIM may increase the risk for liver damage and kidney disease. Thylin et al[45] indicated that SIM may cause clinical symptoms (inflammation) when applied locally in high concentrations. Several researchers have studied local delivery of statins to increase bone healing and reported that statins have local beneficial effects.[46,47] This study showed that daily release of SIM in the range of 0.02–0.53 μg/day enhances tendon-to-bone in tunnel and does not cause an obvious inflammatory response, as demonstrated by a histologic study (Figure 7).

In an in vivo study, the mechanical properties in the SIM/COL/PET group were significantly greater than that in the control group. SIM can promote tendon–bone healing and bone infiltration into the tendon–bone gap at an early stage of ACL reconstruction. The histological results demonstrated that angiogenesis was achieved in the SIM/

COL/PET group but was rarely observed in the PET control group. These results suggest that SIM/collagen coating not only enhanced osteogenesis but also significantly stimulated neovascularization. In a study by Maeda et al,[19] SIM increased the expression of VEGF, a major angiogenic factor that regulates the growth of new capillaries. The cooperative effects on osteogenesis and vascularization may lead to improved tendon–bone healing.

There are some limitations in this study. We merely investigated whether the properties of SIM could promote tendon–bone healing and did not investigate the pharmacological mechanism. The model of ACL reconstruction of this experiment is New Zealand White rabbits. In the future study, we will focus on optimizing the model of ACL reconstruction (large animals), and more data will be needed.

Conclusion

In summary, we developed a SIM/collagen coating that not only could promote PET artificial ligament histocompatibility and osseointegration but also reach the "ligamentization", as well as suppress osteoarthritis occurrence. SIM can retain its bioactivity, achieve a sustained release, and induce osteogenic differentiation of BMSCs using the strategy presented in this study. This approach offers a potential solution to solve the problem of poor biological properties of artificial ligaments in future applications. We suggest that SIM/collagen-coated PET grafts may be an ideal candidate for ligament reconstruction in the future.

Acknowledgments

Disclosure

The authors declare no conflicts of interest in this work.

References

1. Moses B, Orchard J, Orchard J. Systematic review: annual incidence of ACL injury and surgery in various populations. *Res Sports Med*. 2012;20(3–4):157–179.
2. Mall NA, Chalmers PN, Moric M, et al. Incidence and trends of anterior cruciate ligament reconstruction in the United States. *Am J Sports Med*. 2014;42(10):2363–2370.
3. Kiapour AM, Murray MM. Basic science of anterior cruciate ligament injury and repair. *Bone Joint Res*. 2014;3(2):20–31.
4. Murawski CD, van Eck CF, Irrgang JJ, et al. Operative treatment of primary anterior cruciate ligament rupture in adults. *J Bone Joint Surg Am*. 2014;96(8):685–694.
5. Markatos K, Kaseta MK, Lallos SN, et al. The anatomy of the ACL and its importance in ACL reconstruction. *Eur J Orthop Surg Traumatol*. 2013;23(7):747–752.
6. Kim HS, Seon JK, Jo AR. Current trends in anterior cruciate ligament reconstruction. *Knee Surg Relat Res*. 2013;25(4):165–173.
7. Chen CH. Strategies to enhance tendon graft – bone healing in anterior cruciate ligament reconstruction. *Chang Gung Med J*. 2009;32(5):483–493.
8. Nau T, Lavoie P, Duval N. A new generation of artificial ligaments in reconstruction of the anterior cruciate ligament. Two-year follow-up of a randomised trial. *J Bone Joint Surg Br*. 2002;84(3):356–360.
9. Lavoie P, Fletcher J, Duval N. Patient satisfaction needs as related to knee stability and objective findings after ACL reconstruction using the LARS artificial ligament. *Knee*. 2000;7(3):157–163.
10. Gao K, Chen S, Wang L, et al. Anterior cruciate ligament reconstruction with LARS artificial ligament: a multicenter study with 3- to 5-year follow-up. *Arthroscopy*. 2010;26(4):515–523.
11. Guidoin MF, Marois Y, Bejui J, et al. Analysis of retrieved polymer fiber based replacements for the ACL. *Biomaterials*. 2000;21(23):2461–2474.
12. Corsini A, Bellosta S, Baetta R, et al. New insights into the pharmacodynamic and pharmacokinetic properties of statins. *Pharmacol Ther*. 1999;84(3):413–428.
13. Laufs U, Liao JK. Direct vascular effects of HMG-CoA reductase inhibitors. *Trends Cardiovasc Med*. 2000;10(4):143–148.
14. Schachter M. Chemical, pharmacokinetic and pharmacodynamic properties of statins: an update. *Fundam Clin Pharmacol*. 2005;19(1):117–125.
15. Mundy G, Garrett R, Harris S, et al. Stimulation of bone formation in vitro and in rodents by statins. *Science*. 1999;286(5446):1946–1949.
16. Garrett IR, Mundy GR. The role of statins as potential targets for bone formation. *Arthritis Res*. 2002;4(4):237–240.
17. O'Driscoll G, Green D, Taylor RR. Simvastatin, an HMG-coenzyme A reductase inhibitor, improves endothelial function within 1 month. *Circulation*. 1997;95(5):1126–1131.
18. Okura H, Asawa K, Kubo T, et al. Impact of statin therapy on systemic inflammation, left ventricular systolic and diastolic function and prognosis in low risk ischemic heart disease patients without history of congestive heart failure. *Intern Med*. 2007;46(17):1337–1343.
19. Maeda T, Kawane T, Horiuchi N. Statins augment vascular endothelial growth factor expression in osteoblastic cells via inhibition of protein prenylation. *Endocrinology*. 2003;144(2):681–692.
20. Park JB. The use of simvastatin in bone regeneration. *Med Oral Patol Oral Cir Bucal*. 2009;14(9):e485–e488.
21. Garrett IR, Gutierrez GE, Rossini G, et al. Locally delivered lovastatin nanoparticles enhance fracture healing in rats. *J Orthop Res*. 2007;25(10):1351–1357.
22. Mukozawa A, Ueki K, Marukawa K, et al. Bone healing of critical-sized nasal defects in rabbits by statins in two different carriers. *Clin Oral Implants Res*. 2011;22(11):1327–1335.
23. Ezirganli S, Kazancioglu HO, Mihmanli A, et al. The effect of local simvastatin application on critical size defects in the diabetic rats. *Clin Oral Implants Res*. 2014;25(8):969–976.
24. Tai IC, Fu YC, Wang CK, et al. Local delivery of controlled-release simvastatin/PLGA/HAp microspheres enhances bone repair. *Int J Nanomedicine*. 2013;8:3895–3904.
25. Cui Y, Xiaoguang H, Jingying W, et al. Calvarial defect healing by recruitment of autogenous osteogenic stem cells using locally applied simvastatin. *Biomaterials*. 2013;34(37):9373–9380.
26. Jiang J, Wan F, Yang J, et al. Enhancement of osseointegration of polyethylene terephthalate artificial ligament by coating of silk fibroin and depositing of hydroxyapatite. *Int J Nanomedicine*. 2014;9:4569–4580.
27. Yang J, Jiang J, Li Y, et al. A new strategy to enhance artificial ligament graft osseointegration in the bone tunnel using hydroxypropylcellulose. *Int Orthop*. 2013;37(3):515–521.

28. Monteiro N, Martins A, Reis RL, et al. Nanoparticle-based bioactive agent release systems for bone and cartilage tissue engineering. *Regener Ther*. 2015;1:109–118.

29. Yang L, Webster TJ. Nanotechnology controlled drug delivery for treating bone diseases. *Expert Opin Drug Deliv*. 2009;6(8):851–864.

30. Ruszczak Z, Friess W. Collagen as a carrier for on-site delivery of antibacterial drugs. *Adv Drug Deliv Rev*. 2003;55(12):1679–1698.

31. Yun YR, Won JE, Jeon E, et al. Fibroblast growth factors: biology, function, and application for tissue regeneration. *J Tissue Eng*. 2010; 2010:218142.

32. Anderson K, Seneviratne AM, Izawa K, et al. Augmentation of tendon healing in an intraarticular bone tunnel with use of a bone growth factor. *Am J Sports Med*. 2001;29(6):689–698.

33. Kohno T, Ishibashi Y, Tsuda E, et al. Immunohistochemical demonstration of growth factors at the tendon-bone interface in anterior cruciate ligament reconstruction using a rabbit model. *J Orthop Sci*. 2007;12(1): 67–73.

34. Kim HM, Galatz LM, Das R, et al. The role of transforming growth factor beta isoforms in tendon-to-bone healing. *Connect Tissue Res*. 2011;52(2):87–98.

35. Manning CN, Kim HM, Sakiyama-Elbert S, et al. Sustained delivery of transforming growth factor beta three enhances tendon-to-bone healing in a rat model. *J Orthop Sci*. 2011;29(7):1099–1105.

36. Ma CB, Kawamura S, Deng XH, et al. Bone morphogenetic proteins-signaling plays a role in tendon-to-bone healing: a study of rhBMP-2 and noggin. *Am J Sports Med*. 2007;35(4):597–604.

37. Wang CK, Ho ML, Wang GJ, et al. Controlled-release of rhBMP-2 carriers in the regeneration of osteonecrotic bone. *Biomaterials*. 2009; 30(25):4178–4186.

38. Benglis D, Wang MY, Levi AD. A comprehensive review of the safety profile of bone morphogenetic protein in spine surgery. *Neurosurgery*. 2008;62(5 suppl 2):ONS423–ONS431. [discussion ONS431].

39. Song C, Guo Z, Ma Q, et al. Simvastatin induces osteoblastic differentiation and inhibits adipocytic differentiation in mouse bone marrow stromal cells. *Biochem Biophys Res Commun*. 2003;308(3):458–462.

40. Papadimitriou K, Karkavelas G, Vouros I, et al. Effects of local application of simvastatin on bone regeneration in femoral bone defects in rabbit. *J Craniomaxillofac Surg*. 2015;43(2):232–237.

41. Zhou Y, Ni Y, Liu Y, et al. The role of simvastatin in the osteogenesis of injectable tissue-engineered bone based on human adipose-derived stromal cells and platelet-rich plasma. *Biomaterials*. 2010;31(20): 5325–5335.

42. Pauly S, Luttosch F, Morawski M, et al. Simvastatin locally applied from a biodegradable coating of osteosynthetic implants improves fracture healing comparable to BMP-2 application. *Bone*. 2009;45(3): 505–511.

43. Baek KH, Lee WY, Oh KW, et al. The effect of simvastatin on the proliferation and differentiation of human bone marrow stromal cells. *J Korean Med Sci*. 2005;20(3):438–444.

44. Maeda T, Matsunuma A, Kurahashi I, et al. Induction of osteoblast differentiation indices by statins in MC3T3-E1 cells. *J Cell Biochem*. 2004;92(3):458–471.

45. Thylin MR, McConnell JC, Schmid MJ, et al. Effects of simvastatin gels on murine calvarial bone. *J Periodontol*. 2002;73(10):1141–1148.

46. Lee Y, Schmid MJ, Marx DB, et al. The effect of local simvastatin delivery strategies on mandibular bone formation in vivo. *Biomaterials*. 2008;29(12):1940–1949.

47. Skoglund B, Aspenberg P. Locally applied simvastatin improves fracture healing in mice. *BMC Musculoskelet Disord*. 2007;8:98.